2011 American Control Conference
on O'Farrell Street, San Francisco, CA, USA
June 29 - July 01, 2011

Tumor Irrigation Model for Virotherapy Cancer Treatment

Ricardo Dunia and Thomas F. Edgar

Abstract— **A novel virotherapy cancer model based on tumor capillarity irrigation is proposed and compared to previous developed models. The proposed model consists of blood irrigation layers distributed radially along the tumor and attached to a common blood circulation compartment. It also considers the immune system cell generation and consumption in the blood circulation compartment and its propagation inside the tumor boundary. The model equilibrium conditions result in a quadratic function for which the tumor radius reaches steady state under virotherapy. Such a condition permits determination of the minimum drug dose required to halt the cancer growth. This novel model has great potential for advanced controllers because therapy dose delivery and immune system measurements can actually be applied at the blood compartment.**

I. INTRODUCTION

Viruses that selectively replicate in tumor cells have recently demonstrated their potential use in cancer treatment [1][2]. These viruses, known as oncolytic viruses, are genetically altered to infect and reproduce inside the confined tumor mass without affecting the surrounding organs. An oncolytic virus consists of tumor-tropic RNA, which will only permit the virus to grow inside cells with a defective antiviral response system, in particular cells that lack a functional interferon response. Among the oncolytic viruses with potential use for virotherapy are the adenovirus Onyx-015 [3], the herpes simplex virus HSV-1 [4] and the Newcastle disease virus, NDV [5].

Although analysis of lab results indicates that virotherapy has a very promising future for cancer treatment, there are several factors that could diminish its effectiveness. Among these factors is the development of undesirable immune responses that attack the oncolytic virus inside the tumor [6]. The innate immune system can destroy not only free virus particles but also infected tumor cells, which enables the tumor growing process. Therefore, immune suppression drugs like cyclophosphamide (CPA) have been used in conjunction with Oncolytic viruses in order to maintain the effectiveness of virotherapy during cancer treatment [7]. The delivery and blood concentration of such drugs is also limited to avoid the eradication of the immune system and the development of diverse infections in treated patients [8].

Mathematical models for cancer treatment have contributed to the development of therapy protocols, tumor growth predictions and planning of cancer therapy [9] [10] [11] [12] [13], especially for radiation treatment [14] [15] [16] and chemotherapy [17] [18]. Two tumor dynamic models have been recently developed to study the effectiveness of virotherapy in conjunction with immune suppression treatment. The first model, developed by Friedman et. al [6] and analyzed by Wang and Tian, [19] considers a convective radial migration of immune system cells along the solid tumor. This model is referred to as convective immunization, and it is based on the assumption that immune cells are large enough to be considered part of the tumor mass. A second model developed by Tao and Guo [20] considers the immune cells to be small enough to penetrate and migrate by diffusion inside the tumor mass. Although the virus diffusivity is one order of magnitude larger than the immune cell diffusivity, migration by diffusion is governed by concentration gradients. Therefore, for the diffusion model, the space occupied by immune cells plays no role in the tumor volume.

This study proposes a novel virotherapy model based on tumor irrigation, where the immune cell dynamics take place outside the tumor mass and the immune suppression drug is applied at the bloodstream level. The immune system dynamics as well as the immune suppression drug are applied at the blood compartment attached to the tumor irrigation layers. The concept of immunization by irrigation is introduced here to make the application of the immunization model at the blood compartment realistic.

This paper is organized as follows: Section II provides the description and mathematical formulation of the irrigation model. In Section III the simulation response is analyzed to provide the effect of treatment and to measure the therapy progress. Section IV compares the irrigation model with the convection and diffusion models available in the literature in view of cancer treatment effectiveness. Conclusions and future work are provided in Section V.

II. IRRIGATION MODEL

A. Model Description

The immune system response consists mainly of four phases: recognition, amplification of defense, attack and suppression. Some of these phases take place outside the tumor boundary. Body organs like the bone marrow and the thymus are the main producers of immune cells. Other organs like the spleen produce large amounts of antibodies to fight against antigens, and lymph nodes filter the antigens to evoke a full-fledged immune response. Therefore, it is natural to consider that the dominant dynamics of the immune system response and the application of CPA are connected at the blood level compartment that irrigates the tumor. Therefore, the virotherapy irrigation model is developed to make viable

Ricardo Dunia and Thomas F. Edgar are with the Chemical Engineering Department at the University of Texas at Austin, Austin, TX 78712, USA rdunia@che.utexas.edu and tfedgar@che.utexas.edu

978-1-4577-0079-8/11/$26.00 ©2011 AACC

TABLE I

MODEL PARAMETERS FROM FRIEDMAN ET AL. [6]. THE ABBREVIATION 'VAR' INDICATES THAT THE PARAMETER CHANGES DEPENDING ON THE CASE IN STUDY.

D_v	Virus diffusivity coefficient	$3.6 \times 10^{-2} mm^2/h$
D_z	Immune cell diffusivity coefficient	3.6×10^{-4}
k	Immune killing rate	$2.0 \times 10^{-8} mm^3/h$
k_0	Take-up rate of viruses	$10^{-8} mm^3/h$
P	Cyclophosphamide concentration	var
s	Stimulation rate by infected cells	$56 \times 10^{-8} mm^3/h$
U	Radial tumor cell velocity	var
w	Clearance rate of immune cells	$20 \times 10^{-8} mm^3/h$
β	Infection rate	var
γ	Clearance rate of viruses	$2.5 \times 10^{-2} h^{-1}$
δ	Infected cell lysis rate	$5.6 \times 10^{-2} h^{-1}$
θ	Density of tumor cells	$10^6 cells/mm^3$
λ	Proliferation rate of tumor cells	$2 \times 10^{-2} h^{-1}$
μ	Removal rate of necrotic cells	$2.1 \times 10^{-2} h^{-1}$
τ_e	Blood circulation time constant	$50h$
τ_t	Tumor time constant	$1h$

the application of CPA and its interaction with the immune system at the bloodstream level.

The variables used to describe the tumor progress and its interaction with the oncolytic virus and the immune system are:

- The volumetric fraction of uninfected tumor cells, X: this fraction represents the major cause of tumor enlargement and cancer metastasis. Cancer therapy should maintain X at a low value during treatment.
- The volumetric fraction of infected tumor cells, Y: this fraction represents the tumor cells attacked by the virus, which will promote the virus propagation inside the tumor. Infected tumor cells eventually become dead cells.
- The volumetric fraction of dead tumor cells, N: the increase of this fraction tends to slow down the tumor enlargement or reduce the size of the tumor.
- The immune system concentration, Z: this variable is considered a volumetric fraction or a density in the convection or diffusion model, respectively. The immune suppression drug affects Z, which will eventually impact the tumor growth.
- The density of the free virus particles, V: the virus particles are injected in the tumor at the start of the virotherapy treatment. They propagate by diffusion inside the tumor.
- The radial cell velocity, U: the propagation velocity of the tumor cells determines the rate at which the tumor enlarges or shrinks.

The Table I describes the main parameters used for the irrigation model.

B. Mathematical Formulation

The virotherapy mathematical formulation for spherical tumors results in a nonlinear PDE system, with partial derivatives along the radial coordinate ρ. The azimuthal and polar angle coordinates are not considered due to the assumption of radial symmetry, which simplifies the problem without significantly affecting the accuracy of the solution. The size of the tumor is given by $R(t)$, where t represents time. Because the tumor changes its size during treatment, any evaluation of an external boundary condition also changes with time. Nevertheless, this difficulty is overcome by defining the radial coordinate as $r \equiv \frac{\rho}{R(t)}$, where $r = 1$ represents the tumor surface.

The PDE's that define the dynamic response for the quantities X, Y, N, and V are given by

$$\begin{aligned}
\frac{\partial X}{\partial t} + \left(\frac{U - r\dot{R}}{R}\right)\frac{\partial X}{\partial r} &= \lambda X - \beta V X - F X \\
\frac{\partial Y}{\partial t} + \left(\frac{U - r\dot{R}}{R}\right)\frac{\partial Y}{\partial r} &= \beta V X - k Y Z - \delta Y - F Y \\
\frac{\partial N}{\partial t} + \left(\frac{U - r\dot{R}}{R}\right)\frac{\partial N}{\partial r} &= k Y Z + \delta Y - \mu N - F N
\end{aligned}$$

$$\frac{\partial V}{\partial t} - \left(\frac{r\dot{R}}{R} + \frac{2D_v}{R^2 r}\right)\frac{\partial V}{\partial r} - \frac{D_v}{R^2}\frac{\partial^2 V}{\partial r^2} = \delta Y - k_0 V Z - \gamma V$$

where

$$\frac{1}{Rr^2}\frac{\partial}{\partial r}\left(r^2 U\right) = F$$

and

$$F = \lambda X - \mu N \tag{1}$$

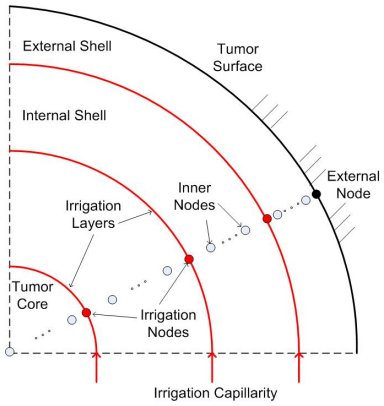

Fig. 1. Irrigation model for virotherapy. The immune system cells circulate in the blood stream and reach the interior of the tumor through blood irrigation capillarity. Irrigation layers are placed in predefined node locations, and immune cells migrate from irrigation layers to the tumor inner tissue by diffusion.

The main differentiator of the irrigation model when compared to the convection and diffusion models is the treatment of the immune system dynamics. The virotherapy irrigation model partitions the spherical tumor into shells and relocates the generation of immune system cells to the blood circulation level. Figure 1 illustrates the notion of an irrigated tumor divided into spherical shells. Inner tumor shell compartments have both faces exposed to irrigation layers. The core inner portion of the tumor is equivalent to a

spheroid, while the most external tumor shell is exposed to an immune cell surface density, Z_R. The location of the tumor determines the boundary value Z_R. The immune system cells migrate from the blood irrigation layers to the inner tumor tissue by diffusion.

The irrigation layers are a subset of the actual nodes used for the calculation of radial profiles. These irrigation layers or nodes are considered in contact with the bloodstream. For convenience, in this work the nodes are equally distributed along the tumor radius. However, in a more general framework, the nodes can be distributed to match the actual location of the tumor capillarity layers.

The partial differential equation for the immune cell density at the irrigation nodes is given by:

$$\frac{\partial Z}{\partial t} - \left(\frac{r\dot{R}}{R} + \frac{2D_z}{R^2 r} \right) \frac{\partial Z}{\partial r} - \frac{D_z}{R^2} \frac{\partial^2 Z}{\partial r^2} = -\frac{(Z - Z_e)}{\tau_t} \quad (2)$$

where Z_e is the immunization density at the blood stream. The time constant τ_t is in the order of one hour and determines the rate at which the irrigation node density Z is impacted by the blood stream density, Z_e.

A diffusion expression, like the one obtained for the diffusion model, governs the migration of the immunization cells to the non-irrigated nodes,

$$\frac{\partial Z}{\partial t} - \left(\frac{r\dot{R}}{R} + \frac{2D_z}{R^2 r} \right) \frac{\partial Z}{\partial r} - \frac{D_z}{R^2} \frac{\partial^2 Z}{\partial r^2} = 0 \quad (3)$$

This type of model considers no generation or suppression of the immune system inside the tumor. Such effects take place in the innate blood stream compartment outside the tumor confinement, and directly impact the immune cell density rate of change at the blood stream level,

$$\tau_e \frac{dZ_e}{dt} = [s\hat{Y} - w(Z_e - Z_n) - P(t)]Z_e \quad (4)$$

where Z_n represents the nominal immune cell density at the bloodstream compartment in the absence of tumor cells and immune suppression drugs. Such a parameter indicates a minimum immunization cell density at the bloodstream level during normal conditions. The time constant τ_e is on the order of 50hr, typical for the time required by CPA to impact the immune system. The average infected cell fraction $\hat{Y}$ is used in the place of the local fraction Y to account for an overall effect of the infected cells on the immunization system generation. A more complete mechanism should include the recognition and amplification of the immune system cells in the bloodstream due to the presence of infected tumor cells. Nevertheless, such a mechanism has been significantly simplified to compare the models presented in this paper using equivalent generation and suppression parameters.

C. Equilibrium Conditions

The equilibrium condition expressions based on the irrigation model for $Z(R) = Z_e$ are given by:

$$\bar{Y} = \frac{\bar{V}(w\gamma - k_0 P + k_0 w Z_n)}{w\delta - k_0 s\bar{V}} \quad (5)$$

$$\bar{Z} = \bar{Z}_e \quad (6)$$

$$\bar{Z}_e = \frac{s\bar{V}\gamma - P\delta + wZ_n\delta}{w\delta - k_0 s\bar{V}} \quad (7)$$

where,

$$\bar{V} = (\lambda - \bar{F})/\beta \quad (8)$$

$$\bar{X} = \frac{\bar{Y}(k\bar{Z} + \delta + \bar{F})}{\beta\bar{V}} \quad (9)$$

$$\bar{N} = 1 - \bar{X} - \bar{Y} \quad (10)$$

The condition $\bar{F} = 0$ provides the following quadratic polynomial form in terms of P,

$$aP^2 + bP + c = 0 \quad (11)$$

where the polynomial coefficients are given by

$$\begin{aligned} a &= kk_0\beta\delta(\lambda + \mu) \\ b &= -k(2k_0 w Z_n \beta\delta + w\beta\gamma\delta + k_0 s\gamma\lambda)(\lambda + \mu) + \\ &\quad k_0(-w\beta\delta + k_0 s\lambda)(\lambda\mu + \delta(\lambda + \mu)) \\ c &= -{k_0}^2 s^2 \lambda^2 \mu + w^2\beta\delta(-\beta\delta\mu + \gamma(\lambda\mu + \delta(\lambda + \mu))) + \\ &\quad sw\lambda\left(k\gamma^2(\lambda + \mu) - k_0(-2\beta\delta\mu + \gamma(\lambda\mu + \delta(\lambda + \mu)))\right) \end{aligned}$$

The substitution of the parameter values of Table I in the expressions above give

$$a(\beta) = 0.005143\beta \quad (12)$$

$$b(\beta) = -0.6102(\beta - 0.137) \quad (13)$$

$$c(\beta) = -2.95(\beta - 7.7014)(\beta - 0.3181) \quad (14)$$

The Static Line (SL) in Fig.(2) represents the solution of the quadratic polynomial in Eq.(11) for different β. Points to the right of SL ($\bar{F} < 0$) define treatment conditions in which the tumor shrinks in time, while the region to the left of SL ($\bar{F} > 0$) represents treatment conditions for tumor enlargement. Points { A, B, C } show the progress from tumor enlargement ($\bar{F} = 0.5$) to tumor reduction ($\bar{F} = -0.5$) by increasing β and keeping $P = 4$. Point B is at the SL and represents the response for $\beta = 6.88$, which makes the tumor reach a constant radius $\bar{R} \neq 0$ after several days of treatment. The assumption of a nominal density $Z_n > 0$ increases the requirements for larger β in the irrigation model, as is demonstrated in Section IV.

III. SIMULATION RESULTS

The dynamic responses for the tumor radius at points { A, B, C } in Fig.(2) are illustrated in Fig.(3). Although these points share the same immune suppression drug delivery, their β values of { 5.61, 6.88, 8.694 } make the responses significantly different. The addition of the bloodstream compartment in the irrigation model increases the time required for the CPA dose to affect the immune system, which will

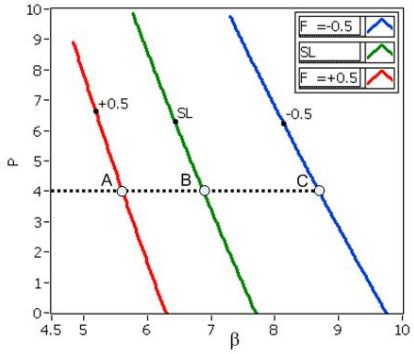

Fig. 2. Static Line (SL) for the irrigation model as a function of the infection rate parameter, β. Point A is at the left of SL, which indicates tumor enlargement. The contrary occurs at the right of SL (point C), where the tumor shrinks after some hours of treatment. Points at the SL (like point B) prevent tumor enlargement by keeping the tumor size constant after days of treatment.

eventually improve the virus replication. A delay term was introduced in the diffusion model presented by Tao [20] to account for the length of time it takes for P to have an effect in the immune system, Z. The irrigation model takes into account such an effect by bringing the generation and attenuation of the immune system to a blood compartment.

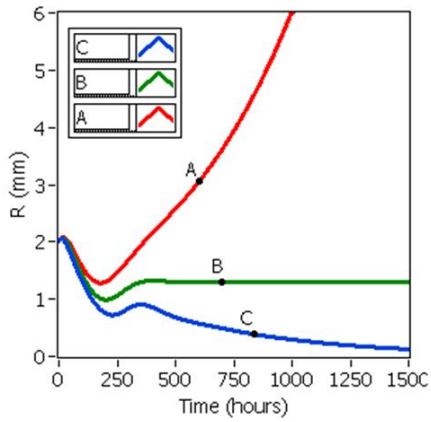

Fig. 3. Tumor radius dynamic responses at points { A, B, C } of Fig. (2).

Stability analysis for the cell fraction dynamics is achieved by linearizing the irrigation model around feasible equilibrium conditions. Figure 4 shows negative real part eigenvalues for the linearized system along the feasible range of β. Such a result indicates stable dynamic responses along SL. A complex pair of eigenvalues is also present in the irrigation model, which makes the response oscillate as shown in Figure 3.

Stable dynamic responses indicate that Eqs. (5) to (7) provide stable cell equilibrium fractions and immune system density. Figure 5 illustrates such steady state values for SL. Controllability conditions were verified along SL. Furthermore, the immune cell density in the blood stream (Z_e) can be measured and used to estimate the remaining states in the irrigation model. Using this measurement, the remaining states proved to be observable along SL. This result indicates

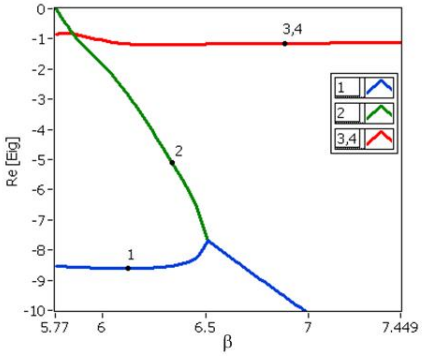

Fig. 4. Eigenvalues (real part) for the linearized model around points along the SL in Figure 2.

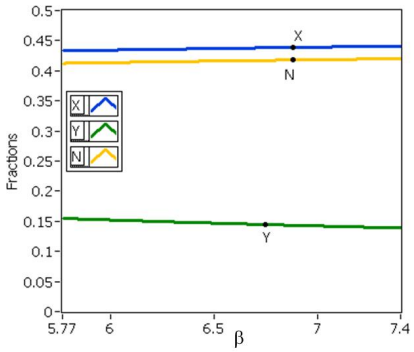

Fig. 5. Tumor cell steady state fractions for the irrigation model along SL.

the potential use of Z_e measurements to estimate the tumor cells' fractions in order to find an optimal treatment.

The next section compares the proposed immune cell migration model based on the virotherapy treatment effect on the cancer growth.

IV. VIROTHERAPY MODEL COMPARISON

The different model assumptions may impact the predicted success of virotherapy. Therefore, it is important to compare them in order to determine which assumption gives the most beneficial result based on the following treatment aspects:

- The relative location of the Static Lines, which determines the amount of CPA required to avoid tumor growth for a given β.
- The dynamic response time, which establishes the response time for treatment progress.
- The reduction of metastasis risk, which determines the chances of cancer propagation in other areas of the host body.

The comparison will determine optimistic and pessimistic predictions for tumor treatment. Furthermore, the fact that convection, diffusion and irrigation models share equivalent model parameters helps to determine the effect of the different immune system cell migration in the effectiveness of cancer treatment.

A. CPA Dose Requirements

A consistent way to compare the immune suppressive drug requirement for the different models is by plotting the static lines of each model on the same graph. Figure 6 illustrates how the SL of the convection model tends to require larger doses of CPA than in the diffusion and irrigation models. These last two models have a very similar SL profile shifted by a constant value $\Delta\beta = 0.22$. Such a small difference is due to the nominal immune suppressive drug density in the blood stream, $Z_n = 0.06$.

Low CPA doses for the diffusion model indicate that the immune suppression drug is more effective when the immune system cells migrate by a diffusion mechanism. The immune cell diffusivity D_z was made two orders of magnitude lower than the virus diffusivity coefficient, D_v. Such an assumption is in accordance with Tao [20], but might have reduced drastically the effectiveness of the immune system for the diffusion model.

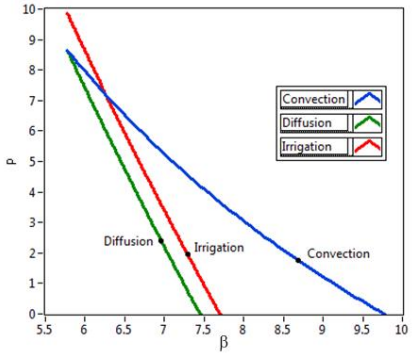

Fig. 6. Comparison of the convection, diffusion and irrigation Static Lines.

In terms of the shape of the $P(\beta)$ function that defines the SL plots, the diffusion and irrigation lines have steeper profiles than the convection one. Steep SL profiles indicate that the same $\Delta\beta$ results in larger changes in P for the diffusion and irrigation models when compared to the convection model. Such a characteristic makes the cancer more difficult to control under the diffusion and irrigation models than with the convection model.

B. Treatment Response Time

Treatment response time is related to the effectiveness of virotherapy in reducing the tumor size. For that reason, a treatment point to the right of SL is considered for all three models. The treatment point under consideration is given by $\beta = 7$ and $P = 8$ as it lies to the right of the SL for all three models. Such a condition allows comparison of radial size reduction using the same infection rate and drug delivery. Figure 7 shows the phase diagram for all three models with time stamp locations for 100, 500, 1000 and 1500 hours of treatment. The colored dots used for each model tend to be close to each other at every time stamp considered in the figure. Nevertheless, differences can be appreciated, and the diffusion model shows the most favorable progress in tumor reduction size. It is important to mention that even though the equilibrium region seems to represent a small portion of the response in the phase diagram, it becomes more than half of the virotherapy treatment in time domain because the last 750 hrs of therapy occur inside the equilibrium region.

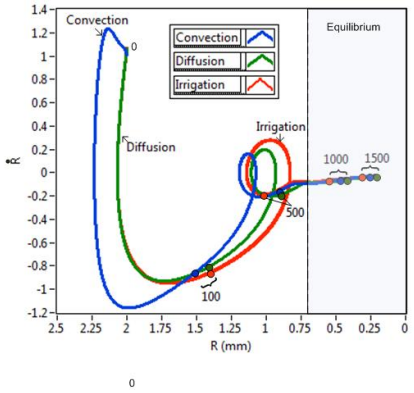

Fig. 7. Phase diagram comparison for the convection, diffusion and irrigation models with time stamp locations of 100, 500, 1000 and 1500 hours of treatment. Equilibrium conditions are achieved after 750 hrs of treatment.

C. Risk of Metastasis

The risk of having metastasis is proportional to the fraction of uninfected tumor cells, X. Therefore, it is important to keep this fraction low during treatment and reduce oscillations that could spark metastasis. The equilibrium fractions provide the final values for the fraction X, while phase diagrams are useful to determine the magnitude of the response oscillations that are detrimental for cancer propagation.

Figure 8 compares $\bar{X}$ for the different models along SL. The equilibrium fractions of uninfected cells seem to be lowest for the convection model along SL. Irrigation and diffusion models share the same equilibrium fractions because the equations that describe their equilibrium conditions are similar. Furthermore, the larger β is, the larger $\bar{X}$ is for the irrigation and diffusion models. The contrary happens in the convection model, where large β values provide lower $\bar{X}$. Therefore, the convection model gives more favorable results to prevent metastasis than the diffusion and irrigation models.

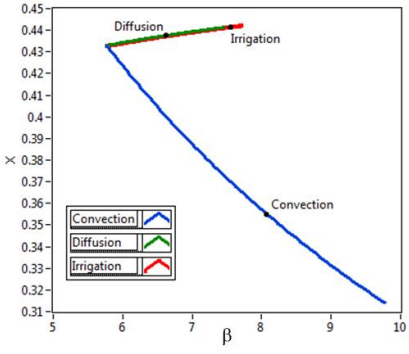

Fig. 8. Uninfected equilibrium fraction for the convection, diffusion and equilibrium models along SL.

A second way to determine the effectiveness of the virotherapy in reducing metastasis is by looking at the oscillations in the phase diagram defined by $\hat{X}(t)$ vs. $R(t)$. Figure 9 shows that the tumor radius under the convection model has the slowest initial response to the treatment because it goes well above the tumor initial radius of 2mm. Nevertheless, the treatment is very effective at reducing $\hat{X}(t)$ as soon as the virotherapy starts for all three models. The largest oscillation occurs for the irrigation model at close to 250 hrs of treatment, where $\hat{X}(t)$ reaches values above 0.65. Therefore, the irrigation model tends to predict larger chances of metastasis that the other two models.

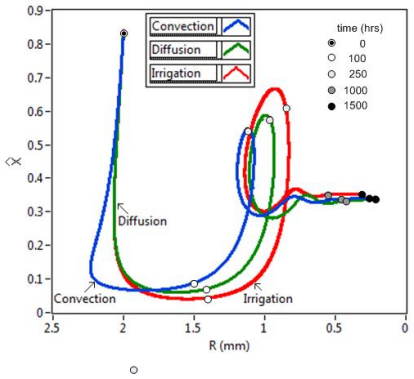

Fig. 9. $\hat{X}(t)$ vs. $R(t)$ phase diagram comparison for $P = 8$ and $\beta = 7$. The irrigation model predicts large oscillations in $\bar{X}$.

V. CONCLUSIONS

An irrigation model is developed in this paper to account for the effect of the innate bloodstream compartment. This blood compartment is where generation and consumption of immune cells occurs, and it interacts with the tumor cells by means of irrigation layers. Such layers are distributed along the spheroidal tumor and partitions it into shells. This model scheme permits the application of the immune suppression drug as well as the measurement of the immune cell density at the bloodstream level. Such aspects provide a realistic view of the virotherapy treatment estimation and control, where the drug delivery takes the place of the manipulated variable and the immune system cell density represents the measured variable. Stability, controllability and observability properties were verified in a linearized model around equilibrium points.

Convection, diffusion and irrigation models were compared to determine the effect of virotherapy treatment under the different model assumptions. There is no major discrepancy among the models, as these adjust accordingly to experimental data collected from animal labs. However, the irrigation model accounts for possible adjustable and measurement variables taken at the bloodstream level, which allows continuous monitoring and control action. Advanced control techniques should account for constraints related to the maximum drug concentrations allowed in the blood circulation system as well as minimum acceptable levels of immune system density. This last constraint should be strongly enforced to avoid the proliferation of harmful infections during cancer treatment.

VI. ACKNOWLEDGMENTS

The authors acknowledge the guidance given by Dr. Marisol Fernandez from the infectious disease staff at Dell Children's Hospital in Austin, Texas.

REFERENCES

[1] M. Vaha-Koskela, J. E. Heikkila, A. E. Hinkkanen, Oncolytic viruses in cancer therapy, Cancer Letters 254 (2007) 178–216.
[2] L. M. Wein, J. T. Wu, D. H. Kirn, Validation and analysis of a mathematical model of a replication-competent oncolytic virus for cancer treatment:implications for virus design and delivery, Cancer Research 63 (2003) 1317–1324.
[3] F. Khuri, J. Nemunaitis, I. Ganly, J. Arseneau, I. Tannock, L. Romel, M. Gore, J. Ironside, R. MacDougall, C. Heise, B. Randlev, A. Gillenwater, P. Bruso, S. Kaye, W. Hong, D. Kirn, A controlled trial of intratumoral onyx-015, a selectively-replicating adenovirus, in combination with cisplatin and 5-fluorouracil in patients with recurrent head and neck cancer, Nature Medicine 6.
[4] J. Markert, M. Medlock, S. Rabkin, G. Gillespie, T. Todo, W. Hunter, C. Palmer, F. Feigenbaum, C. Tornatore, F. Tufaro, R. Martuza, Conditionally replicating herpes simplex virus mutant, g207 for the treatment of malignant glioma: results of a phase i trial, Gene Therapy 7.
[5] L. Csatary, G. Gosztonyi, J. Szeberenyi, Z. Fabian, V. Liszka, B. Bodey, C. Csatary, Mth-68/h oncolytic viral treatment in human high-grade gliomas, Journal of Neuro-Oncology 67.
[6] A. Friedman, J. P. Tian, G. Fulci, E. A. Chiocca, J. Wang, Glioma virotherapy: Effects of innate immune suppression and increase viral replication capacity, Cancer Research 66 (4) (2006) 2314–2319.
[7] H. Wakimoto, G. Fulci, E. Tyminski, E. A. Chiocca, Altered expression of antiviral cytokine mrnas associated with cyclophosphamide's enhancement of viral oncolysis, Gene Therapy 11 (2004) 214–223.
[8] H. Vladar, J. Gonzalez, Dynamic response of cancer under the influence of immunological activity and therapy, Journal of Theoretical Biology 227 (2004) 335–348.
[9] W. Duchting, T. Ginsberg, Computer simulation applied to radiation therapy in cancer research, Applied Mathematics and Computation 74 (1996) 191–207.
[10] W. Duchting, W. Ulmer, T. Ginsberg, Cancer: A challenge for control theory and computer modelling, European Journal of Cancer 32A (8) (1996) 1283–1296.
[11] A. Swierniak, M. Kimmel, J. Smieja, Mathematical modeling as a tool for planning anticancer therapy, European Journal of Pharmacology 625 (2009) 108–121.
[12] R. Araujo, L. McElwain, A history of the study os solid tumour growth: The contribution of mathematical modelling, Bulletin of Mathematical Biology 66 (2003) 1039–1091.
[13] N. F. Kirby, Modeling and simulation of radiotherapy, Nuclear Instruments and Methods in Physics Research B255 (2007) 13–17.
[14] R. Bodey, P. Evans, G. Flux, Application of the linear-quadratic model to combined modality radiotherapy, International Journal of Radiation Oncology 59 (1) (2003) 228–241.
[15] N. F. Kirby, N. G. Burnet, D. B. F. Faraday, Mathematical modeling of the response of tumour cells to radiotherapy, Nuclear Instruments and Methods in Physics Research B188 (2002) 210–215.
[16] A. Ergun, K. Camphausen, L. Wein, Optimal scheduling of radiotherapy and angiogenic inhibitors, Bulletin of Mathematical Biology 65 (2003) 407–424.
[17] J. Harrold, R. S. Parker, Clinically relevant cancer chemotherapy dose scheduling via mixed-integer optimization, Computers and Chemical Engineering 33 (2009) 2042–2054.
[18] E. S. Norris, J. R. King, H. M. Byrne, Modelling the response of spatially structured tumours to chemotherapy: Drug kinetics, Mathematical and Computer Modeling 43 (2006) 820–837.
[19] J. Wang, J. Tian, Numerical study for a model of tumor virotherapy, Applied Mathematics and Computation 196 (2008) 448–457.
[20] Y. Tao, Q. Guo, The competitive dynamics between tumor cells, a replication-competent virus and an immune response, Journal of Mathematical Biology 51 (2005) 37–74.